JOURNAL OF BACTERIOLOGY, Sept. 2011, p. 4523–4530 Vol. 193, No. 17
0021-9193/11/$12.00 doi:10.1128/JB.00231-11

Helicobacter pylori Possesses Four Coiled-Coil-Rich Proteins That Form Extended Filamentous Structures and Control Cell Shape and Motility▽

Mara Specht,[2] Sarah Schätzle,[1,2] Peter L. Graumann,[2] and Barbara Waidner[1,2]*

Department of Medical Microbiology and Hygiene, Institute of Medical Microbiology and Hygiene, University Hospital Freiburg, Hermann-Herder-Straße 11, D-79104 Freiburg,[1] and Department of Microbiology, Faculty for Biology, University of Freiburg, Schaenzle Straße 1, 79104 Freiburg, Germany[2]

Received 17 February 2011/Accepted 21 May 2011

We identified two additional genes of *Helicobacter pylori* encoding Ccrp proteins. All four Ccrps have different multimerization and filamentation properties and different types of smallest subunits and do not copurify, suggesting a system of individual Ccrp filaments. Despite the presence of morphologically unaltered flagella, all *ccrp* mutants displayed significantly reduced motility.

Helicobacter pylori is a Gram-negative, highly motile, microaerophilic, spiral-shaped organism, which colonizes the stomachs of at least half of the world's human population (11). The cell shape of *H. pylori* has always been held as an important pathogenicity factor. The cell shape of *H. pylori* is apparently controlled by two unrelated mechanisms that operate at two levels: peptidases influence cell shape by causing peptidoglycan relaxation (5, 26), whereas so-called coiled-coil-rich proteins (Ccrp) compose an intracellular scaffold (30). In *Caulobacter crescentus*, the coiled-coil-rich protein crescentin is essential for the generation of cell curvature (2), likely through mechanical control of cell growth (6). In *Streptomyces coelicolor*, the filament-forming Ccrp FilP determines cell rigidity but not cell shape (4). Recently, Ccrp RsmP was shown to be essential both for viability and for rod shape determination in *Corynebacterium glutamicum* (8). *H. pylori* possesses two Ccrp proteins (Ccrp59 and Ccrp1143), which are essential for the maintenance of proper cell shape (30).

In this work, a close inspection of the genome of *H. pylori* 26695 revealed the presence of genes encoding proteins rich in putative heptad repeat regions, located adjacent to the previously characterized *ccrp59* and *ccrp1143* genes: HP0058 lies upstream of *ccrp59*, and HP1142 lies downstream of *ccrp1143.* This gene arrangement is conserved in all strains analyzed (26695, J99, HAPG1, 1061, G27, and B128). Concerning HP0058, we have identified a sequencing error (creating a wrong annotation) in the presumed intergenic region upstream of gene HP0058: the C stretch at bp position 62013 in the genome of strain 26695 is composed of 17 C's rather than the reported 15 C's. Because of this frameshift, HP0058 begins at bp position 61943, encoding an approximately 48-kDa protein. Indeed, we found that only the long version of HP0058 is expressed in *H. pylori* cells. Based on their putative coiled-coil-rich structure, we designate the *H. pylori* HP0058 and HP1142 gene products Ccrp58 and Ccrp1142, and the genes will be referred to as *ccrp58* or *ccrp1142* here.

Both new *ccrp* genes are also highly heterogenic between *H. pylori* strains (18, 22). It has been suggested that the genes are submitted to specific selection pressure, making them evolve rapidly. By using BLASTn (NCBI) and the sequence of strain 26695 as a reference, the maximum identity of the *ccrp58* and *ccrp1142* genes of all sequenced *H. pylori* strains decreased to 84% and 89%, respectively. However, genes were found in all sequenced strains available. This hypervariability may contribute to the highly different morphologies of *H. pylori* strains.

To study the functions of Ccrp58 and Ccrp1142, we inactivated both genes separately in the *H. pylori* strains 26695 and KE88-3887 (KE) and analyzed their role in cell shape determination. The strains, plasmids, and primers used are listed in Tables 1 and 2. Mutants were derived as described previously (19, 28, 29). Growth analysis of both mutants revealed that the inactivation of either gene affected the growth rate of *H. pylori* (not shown). While less than 15% of 26695 wild-type cells were found to be straight (Fig. 1A), the percentage of straight cells in the population was 50% in the *ccrp58* mutant ($n = 400$) and 40% in the *ccrp1142* mutant ($n = 130$) (Fig. 1B and C). With regard to cell morphology, the corresponding mutants in strain KE behaved similarly (not shown). Because deletion of *ccrp59* leads to the formation of 100% straight cells (30), a polar effect of the *ccrp58* disruption could be excluded.

The gene HP1141 downstream of *ccrp1142* encodes methionyl-tRNA formyltransferase, whose function is essential in some bacteria (3, 10). The deletion of *ccrp1142* produced viable cells without any detectable growth defect, demonstrating that this deletion did not affect the expression of gene HP1141. To specify the effect of these deletions on cell morphology, we used a cell filamentation assay with aztreonam as previously described (26). This inhibitor of the septal peptidoglycan synthesis forces cells into long chains and therefore facilitates the determination of helicity. Accordingly, helical wild-type cells of strain 26695 formed polymorphic spiral chains, without regular pitch (Fig. 1D). Aztreonam-treated *ccrp58* and *ccrp1142* mu-

* Corresponding author. Mailing address: Institut für Med. Mikrobiologie und Hygiene, Hermann-Herder-Str. 11, 79104 Freiburg, Germany. Phone: 49 (0)761 203 6539. Fax: 49 (0)761 203 6562. E-mail: barbara.waidner@uniklinik-freiburg.de.

▽ Published ahead of print on 3 June 2011.

TABLE 1. Plasmids and strains used in this study

Strain or plasmid	Relevant characteristics[a]	Reference or source
Plasmids		
pTn*Max*5	*lacI*^{q} *tnpR tnpA res ori*$_{fd}$ *cat*$_{GC}$, Cm^r	17
pZERO-2	Cloning vector, MCS in *lacZ′ neo*, Km^r	Invitrogen
p0058PCAT	pZERO-2, ΔHP0058::*Pcat*, Cm^r Km^r	This study
p0058StrepPCAT	pZERO-2 carrying 500 bp of the C terminus of HP0058 fused with a Strep tag, a chloramphenicol resistance cassette, and 500 bp of the N terminus of *ccrp59*	This study
p1142PCAT	pZERO-2, ΔHP1142::*Pcat*, Cm^r Km^r	This study
pASK-IBA7	Expression vector, *tetR* P_{tet} *bla*, Ap^r	IBA
pIBA7-1142	pASK-IBA7 carrying the HP1142 coding sequence under the control of the *tet* promoter cloned in the BsaI site	This study
pIBA7-0059	pASK-IBA7 carrying the HP0059 coding sequence under the control of the *tet* promoter cloned in the BsaI site	30
pETDuet-1	*bla*	Novagen
pETDuet-1143	pETDuet-1 carrying the HP1143 coding sequence under the control of the T7promoter cloned between the NcoI and BamHI sites	30
pETDuet-0058	pETDuet-1 carrying the HP0058 coding sequence under the control of the T7promoter cloned between the EcoRI and PstI sites	This study
Strains		
E. coli strains		
BL21	F$^-$ *dcm ompT hsdS*(r_B^- m_B^-) *gal*	Stratagene
BL21-Ccrp58	BL21 carrying plasmid pETDuet-0058	This study
BL21-Ccrp59	BL21 carrying plasmid pIBA7-0059	30
BL21-Ccrp1143	BL21 carrying plasmid pETDuet-1143	30
BL21-Ccrp1142	BL21 carrying plasmid p pIBA7-1142	This study
DH5α	F$^-$ φ80d*lacZ*ΔM15 Δ(*lacZYA-argF*)*U169 deoR recA1 endA1 hsd*R*17*(r_K^- m_K^+) *phoA supE44* λ$^-$ *thi-1 gyrA96 relA1*	Bethesda Research Laboratories
H. pylori strains		
26695	wt, containing the entire *cag* PAI	27
KE88-3887	Piglet-passaged strain 26695	15
KE-Ccrp58Strep	KE88-3887, Ccrp58 fused to Strep tag, Cm^r	This study
KE-59PCAT	KE88-3887, ΔHP0059::*Pcat*, Cm^r	30
KE-1143PCAT	KE88-3887, ΔHP1143::*Pcat*, Cm^r	30
KE-58PCAT	KE88-3887, ΔHP0058::*Pcat*, Cm^r	This study
KE-1142PCAT	KE88-3887, ΔHP1142::*Pcat*, Cm^r	This study
26695-59PCAT	26695, ΔHP0059::*Pcat*, Cm^r	30
26695-1143PCAT	26695, ΔHP1143::*Pcat*, Cm^r	30
26695-58PCAT	26695, ΔHP0058::*Pcat*, Cm^r	This study
26695-1142PCAT	26695, ΔHP1142::*Pcat*, Cm^r	This study

[a] MCS, multiple cloning site; wt, wild type; PAI, pathogenicity island.

tant strains showed a remarkable homomorphous phenotype of almost straight chains (Fig. 1D). This phenotype was more pronounced in the *ccrp58* mutant strain, which is in agreement with the somewhat higher impact of *ccrp58* deletion on cell morphology. Thus, both novel *ccrp* genes play an important role in cell shape maintenance.

Subsequently, we investigated the influence of the deletion of *ccrp* genes on flagellum formation using the fluorescent membrane stain FM4-64 at a final concentration 1 nM (the flagella of *H. pylori* are covered by a membranous sheath [9]). Fluorescence microscopy was performed on a Zeiss Axioplan2 with a digital AxioCam MRm camera (30). However, flagella are not visible in all cells, as they can shear off during the preparation of cells or sit in a focal plane different from that of the cell body. Nevertheless, no defect in flagellum formation was found for any of the *ccrp* mutants (Fig. 1B and C and data not shown). To verify this finding, we analyzed the presence of flagella by transmission electron microscopy using a Philipps/FEI CM10 (80000V) electron microscope (31). Polar flagella were readily visible in the wild type as well as in all *ccrp* mutants (Fig. 1, right, and data not shown). Deletion of *ccrp* genes therefore has no visible effect on the formation of flagella in *H. pylori.* It is believed that the helical shape of *H. pylori* enables the bacteria to penetrate the mucin web in the stomach (1, 24). Because strain 26695 is flagellated but only moderately motile (16), we tested swimming motility in strain KE, which is a highly motile variant of strain 26695, using soft-agar assays (23). We observed that all four *ccrp* mutants had significantly impaired motility (Fig. 2; $P < 0.001$, analysis of variance [ANOVA], Tukey's test). Surprisingly, the level of motility reduction did not strictly correlate with the loss of spiral cell shape. The deletion of the *ccrp59* gene, which leads to 100% straight cells, caused the least pronounced motility defect, whereas the smallest halo diameters were found in the *ccrp58* and the *ccrp1143* mutant strains. Possibly, a rod shape is more advantageous for motility than an irregular helical shape or slight curvature but is less advantageous than a helical shape. Alternatively, Ccrps may be involved in other cellular processes necessary for motility.

Eukaryotic intermediate filament (IF) proteins are involved

TABLE 2. Oligonucleotides used in this study[b]

Gene[a]	Application	Primer	Sequence (5′→3′)
HP0058	Mutagenesis	0058-L3	GCTAACTAACAAGATCACCG
		PCAT-0058-R2	1-CGCTATGAGTTGTTGCTACA
		CAT-0058-L1	2-GCGCTTATGACTATACATGC
		0059-R1	CGGTGATCTTGTTAGTTAGC
HP1142	Mutagenesis	1143-L1	AAGCGACATGCGAGAGATTG
		PCAT-1142-R1	1- CCACTGCTTACATTCTGCTG
		CAT-1142-L1	2- GAAGATGGTCAATTAGTAGG
		1142-R2	TATAATGAGCTTCATGACCG
HP0058	Strep tag fusion	58s-L2	ATGGTAGGTCTCAGCGCTTGTTAAGAGAAAAAGAAAATCTCAATA
		58Strep-PCAT	GGCGGATTAACAAAAACCGGACTATTTTTCAAATTGCGGGTG
		59PCAT	TGGCAGGGCGGGGCGTAAATGGGA
		59_dw	GCTCTTGTTTAAGGCTATCC
HP0058	Expression	58_up	TCAGAATTCATGATGGGTGCTCATATTATAG
		58_Strepdw	TCACTGCTATTTTTCGAACTGCGGGTGGCTCCACCCGCCTGATCCC ATATCCACGATAGT
HP1142	Expression	pASK7-1142-L1	ATGGTAGGTCTCAGCGCGTGAGCGTGAATAGTAATGGCAAT
		pASK7-1142-R1	ATGGTAGGTCTCATATCACTTCATTCTCATCATCATTTTATAATG
Pcat	*cat* gene with promoter	CATS1	TCCGGTTTTTGTTAATCCGCC
		CATAS1	TTACGCCCCGCCCTGCCA

[a] Gene numbers refer to the *H. pylori* 26695 genome sequence (27).
[b] The 5′ extensions used for the fusion of PCR products to the *cat* gene by megaprimer PCR are labeled as follows: 1 (5′-GGCGGATTAACAAAAACCGGA), complementary to the 5′ region of the *cat* gene with promoter; 2 (5′-TGGCAGGGCGGGGCGTAA), complementary to the 3′ end of the *cat* gene. The BsaI restriction site used for the protein expression via the IBA system is underlined.

in intracellular trafficking and positioning of cellular organelles (12). Thus, it may be possible that Ccrp proteins adopt some of these properties in prokaryotic cells. Furthermore, although flagella were clearly visible in the Ccrp mutants, we cannot exclude a possible defect in flagellum motion. Interestingly, cells with mutations in recently identified *H. pylori* genes, which promote the helical cell shape by causing peptidoglycan relaxation, were not or only minimally reduced in their ability to swim directionally in a similar soft-agar assay (5, 26). However, Ccrp proteins of *H. pylori*, besides their function in cell shape maintenance, clearly influence motility.

We purified Ccrps as C- (Ccrp58) or N-terminally (Ccrp1142, Ccrp59, and Ccrp1143) Strep-tagged versions as described previously (30) (plasmids shown in Table 1). Contrarily to IF proteins that are generally insoluble, recombinant versions of all Ccrps could be purified as soluble proteins and were analyzed by gel filtration using either a Superose6 10/300GL column (Tricorn) or a Biosep-SEC-S4000 (Phenomex) in Strep tag washing buffer (buffer-W; IBA GmbH) yielding Stokes radii. Furthermore, we performed sucrose gradient sedimentation experiments using ultracentrifugation (Beckman SW-41 rotor, 13,000 × *g*, 4°C, 15 h) through linear 5 to 15% sucrose gradients. Because Ccrp proteins have been shown to be filamentous (30), the native weight (*M*) must be deduced from the combination of the Stokes radius (Rs) and the sedimentation coefficient using the equation $M = 3.909s \times \mathrm{Rs}$. Accordingly, the calculated native masses of Ccrp58, Ccrp59, Ccrp1142, and Ccrp1143 are 295 kDa, 127.8 kDa, 184 kDa, and 170 kDa, respectively. The smallest units of Ccrp58, Ccrp59, Ccrp1142, and Ccrp1143 are therefore likely a hexamer (annotated molecular mass of 48 kDa), a tetramer (32 kDa), a dimer (88 kDa), and a trimer in solution (50.5 kDa), respectively. Whereas a dimeric structure is a precursor of a tetramer, the trimeric structure is found in collagen and could be seen as a prestage of the hexamer structure. These results demonstrate that *H. pylori* Ccrps have different multimeric single units as building blocks of the filaments. The biochemical properties of all four Ccrps are summarized in Fig. 3.

Interestingly, we observed an increase of large assemblies of Ccrp58 and Ccrp1142 over time (Fig. 4C and D, right), as gel filtration experiments performed with the Biosep-SEC-S4000 column showed that the elution peak of the same sample changed to larger sizes after 2 (Fig. 4C and D, blue curves) and 4 weeks (Fig. 4C and D, green curves), compared to the apparent size derived directly after Strep tag purification (Fig. 4C and D, red curves). Furthermore low-spin centrifugation (13,000 rpm) revealed that Ccrp58 was found mostly in the supernatant at pH 8, whereas decreasing the pH increased sedimentation, and at pH 6, most of Ccrp58 was present in the pellet fraction (Fig. 4A).

Electron microscopy analysis showed that purified Ccrp58 formed filaments with an average length of 50 nm (Fig. 5A) at pH 8. Additionally we could observe some longer filaments of 200-nm length (Fig. 5A, white arrow). A control (buffer E; IBA GmbH) showed a plain gray image without any structure (Fig. 5D). Whereas the addition of up to 10 mM magnesium chloride or calcium chloride had no effect on filament formation, the decrease of the pH from pH 8 to pH 7 resulted in the formation of much longer filaments of up to 1 μm (Fig. 5A right, white arrows) as well as of bundles of filaments (gray arrows). These results demonstrate that the assembly of Ccrp58 is dependent on pH and time, very similarly to the assembly of IF proteins (14).

Ccrp1142 also forms filamentous structures *in vitro*, indepen-

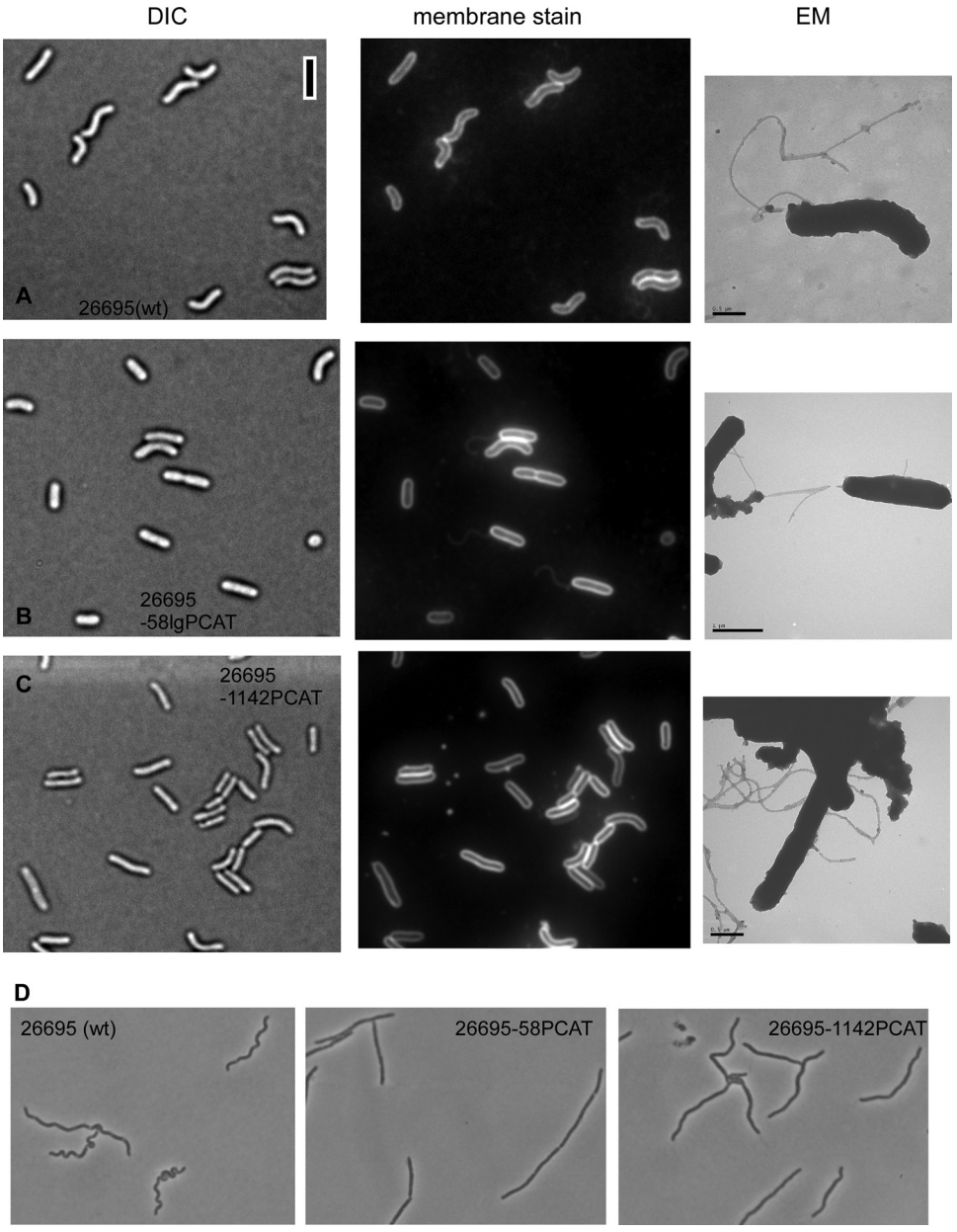

FIG. 1. Analysis of cell morphology of *H. pylori* strain 26695. Wild type (A), *ccrp58* mutant (B), and *ccrp1142* mutant (C). Nomarski DIC images (left), fluorescent micrographs of FM4-64 membrane staining (middle), transmission electron microscopy images of phosphotungstic acid (PTA)-stained cells (right). Wild-type (wt) and mutant strains are indicated in the images. Black bar, 2 μm. All images are equally scaled. (D) Phase contrast of wild-type and mutant cells treated with the filamenting drug aztreonam.

dent of any cofactor (Fig. 5C). In contrast to Ccrp58, but similar to Ccrp59 (30), Ccrp1142 already formed long bundles of filaments (Fig. 5C) at pH 8. Single filaments had a diameter of 10 nm, while the width of whole bundles was more than 100 nm. The length of the bundles could even reach more than 500 nm (Fig. 5C).

To obtain more information on the native architecture of Ccrp58 filaments, we generated a construct in which the 3′ end of *ccrp58* is fused to a Strep tag and an adjacent chloramphenicol resistance cassette (21), and primers listed in Table 2. This construct was integrated into the *ccrp58* locus in strain KE, and correct integration was confirmed by PCR and sequencing. The morphology of the Ccrp58-Strep fusion strain was as spiral as that of wild-type cells, showing that the fusion does not disturb function. Ccrp58-Strep could be efficiently purified from *H. pylori* cell extracts (Fig. 4B) using procedures used for *E. coli* cell extracts (30). Electron microscopy revealed that Ccrp58 was also organized in filaments (Fig. 5B). Interestingly, even when these filaments were purified at pH 8, they were much longer than those observed after purification from *E. coli*. Apparent single filaments had a diameter of about 7 nm, but filaments generally assembled into large bundles with a diameter of about 100 nm and a length of more than 1 μm (Fig. 5B). *H. pylori* wild-type cell extracts

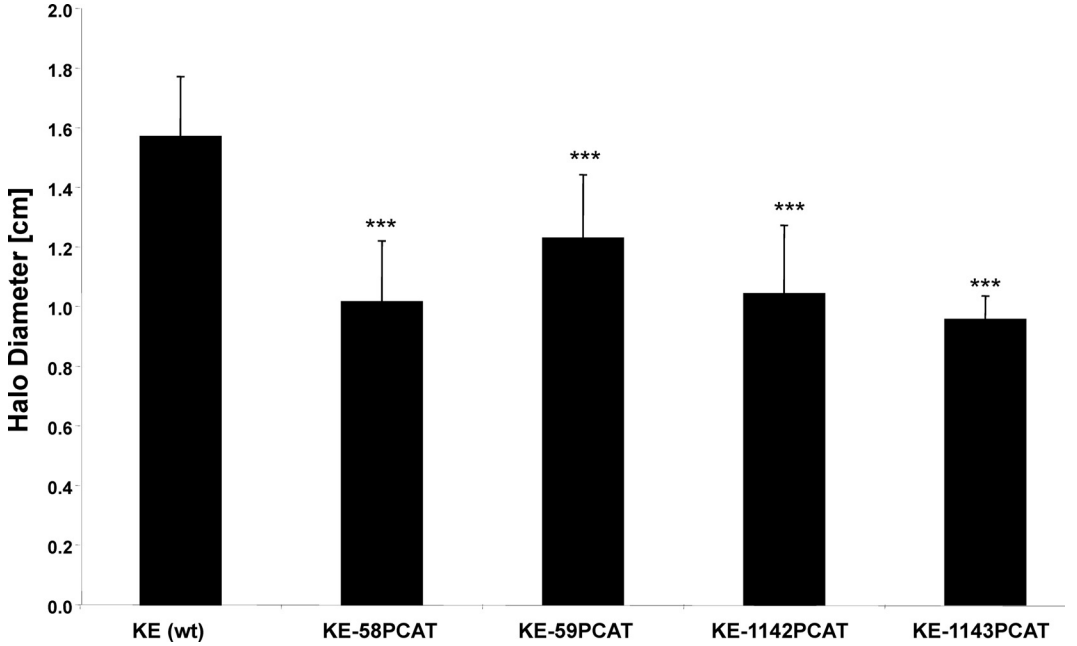

FIG. 2. Motility phenotype of all Ccrp mutants in soft agar depicted as mean halo diameter of at least three independent experiments totaling 200 stabs per strain in soft agar after 5 days. Stars indicate significant differences from wild type ($P < 0.001$, ANOVA with Tukey test).

subjected to Strep tag purification and analyzed by electron microscopy did not show any filamentous structures, indicating that the observed filaments are indeed composed of Ccrp58-Strep (Fig. 5E).

These findings raise several possibilities: the simplest explanation might lie with the internal pH of *E. coli*, which is pH 7.8 (20) and thus similar to the standard purification conditions, whereas the pH in the cytoplasm of *H. pylori* is pH 6.8 (25). Additionally, Ccrp58 could be modified *in vivo*, e.g., phosphorylated, as has been shown for IF proteins, which contain numerous phosphorylation sites involved in their assembly/disassembly and subcellular organization (13). Furthermore, copolymerization of Ccrps could act as facilitation factor. Hence, to address this question we analyzed Ccrp58 eluates from *H. pylori* cells by mass spectrometry (nano-liquid chromatography–tandem mass spectrometry [nLC-MS/MS]) for the presence of the other Ccrp proteins according to the method of Defeu Soufo et al. (7). As a control, extracts from *H. pylori* cells lacking the Strep fusion were run over Strep-tactin columns. Only a small amount of Ccrp1143 could be detected by this comparative analysis within the Ccrp58-Strep eluate. None of the other Ccrp proteins was found to coelute with Ccrp58-Strep. These data suggest that rather than being part of a mixed filamentous structure, Ccrp58 forms individual fila-

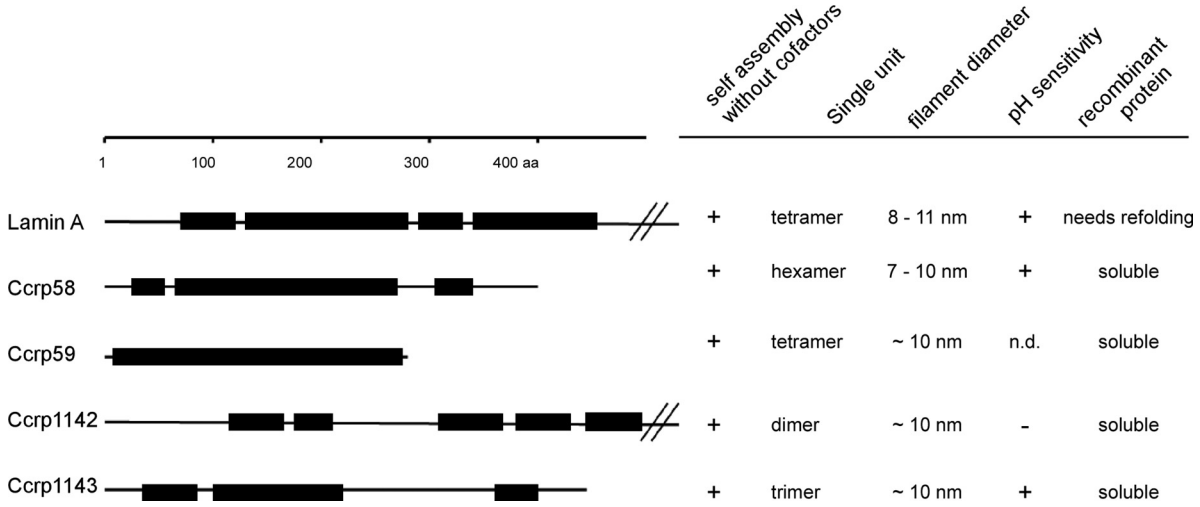

FIG. 3. Architectures and biochemical properties of Ccrp proteins. The tripartite building plan of a human IF protein nuclear lamin A is depicted at the top. The scale bar refers to amino acid residues. Boxes represent domains in coiled-coil conformation and lines noncoiled-coil sequences. Long head or tail domains are in some cases truncated. n.d., not determined.

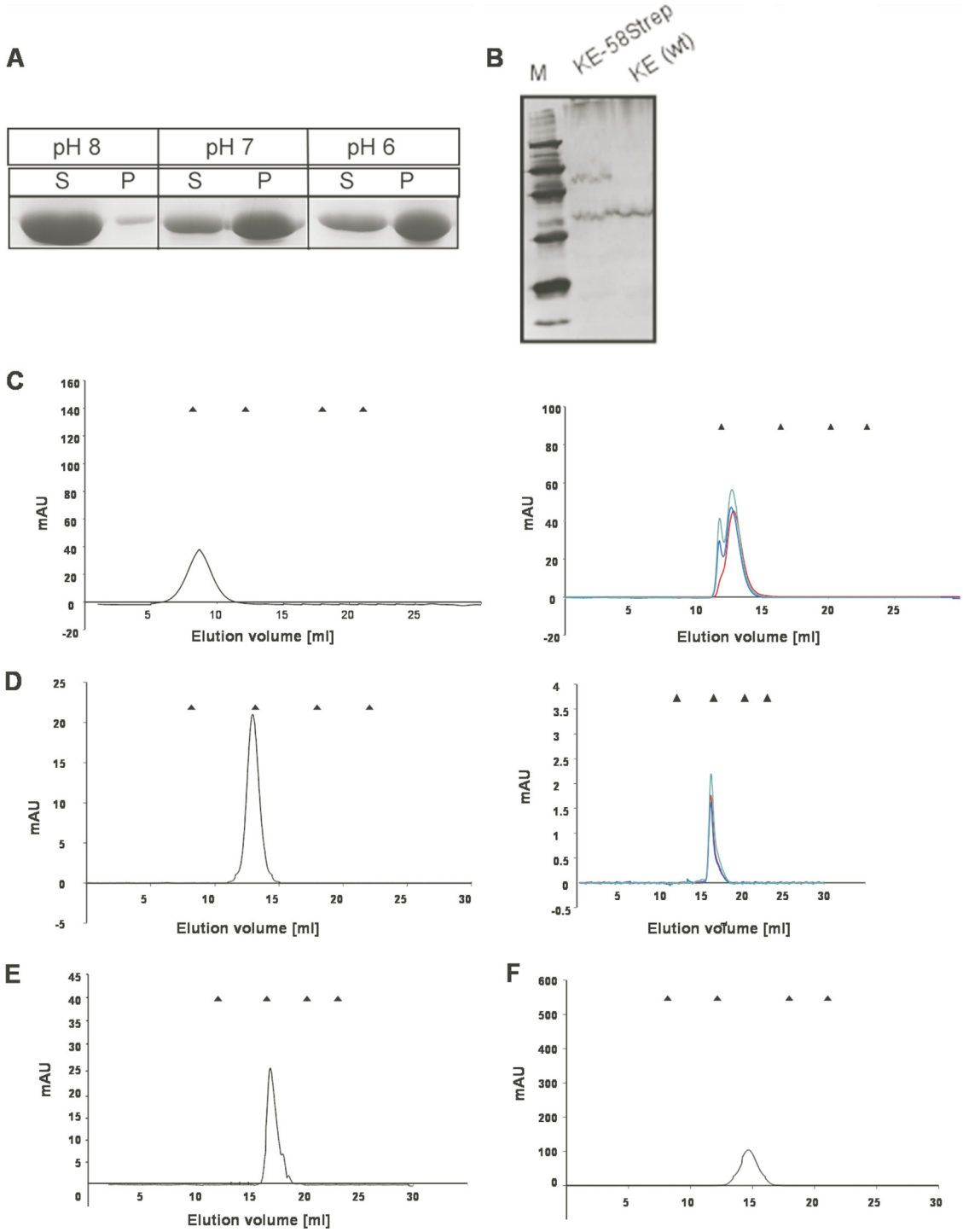

FIG. 4. (A) Spin-down assay of Ccrp58 after purification from *E. coli*. Coomassie-stained SDS-PAGE of spin-down assays of 20-μl fractions. S, supernatants; P, pellets resuspended in 20 μl SDS loading buffer. Different pH levels are indicated. (B) Western blot of 20 μg of whole-cell extracts of *H. pylori* wild-type cells (KE) and of the mutant, in which Ccrp58 is fused to the Strep tag (KE-58Strep) as indicated. M, marker; marker protein sizes are indicated. The antiserum recognizes the tagged version of Ccrp58 in strain KE-58Strep, as well as a nonspecific band, which can also be seen with the parent strain KE. (C to F) Analytical gel filtration of Ccrp proteins. Elution profiles of analytical gel filtration of Ccrp58 (C) and Ccrp1142 (D) using a Superose6 10/300 column (left) and a Biosep-SEC-S4000 column (right). In the right panels, the red curves display gel filtration immediately after purification, the blue curves after 2 weeks, and the green curves after 4 weeks after purification. Elution profiles of Ccrp59 (E) and Ccrp1143 (F) using a Superose6 10/300 column. The triangles above each elution profile indicate the elution times of the standard proteins (Bio-Rad) as follows: thyroglobulin (670 kDa, 19 S), bovine gamma-globulin (158 kDa, 7.4 S), chicken ovalbumin (44 kDa, 3.5 S), equine myoglobin (17 kDa, 2.0 S), vitamin B_{12} (1.35 kDa). mAU, milliabsorbance units.

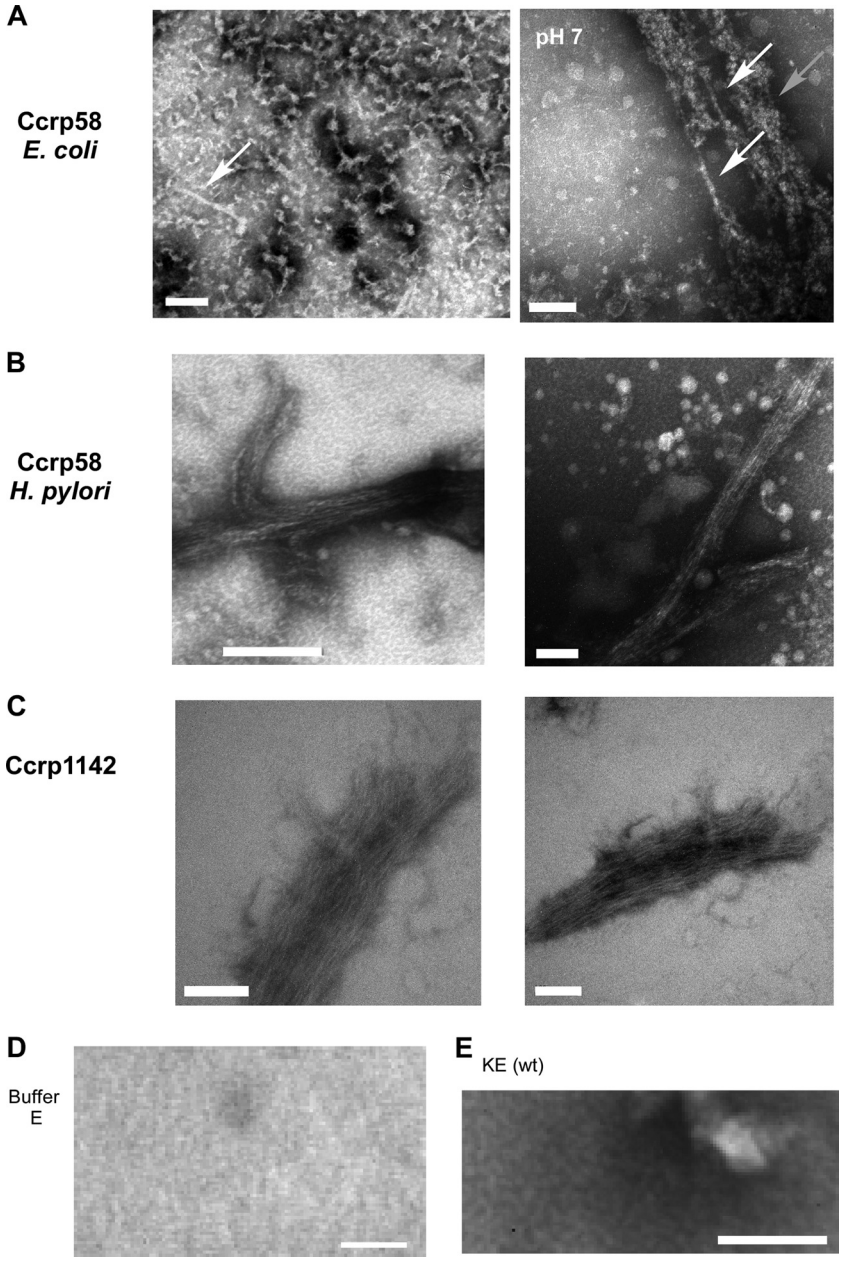

FIG. 5. Electron microscopic images of Ccrp58 and Ccrp1142 purified at pH 8. (A) Ccrp58-Strep expressed in *E. coli*. White arrows indicate single long filaments, and gray arrow indicates a bundle of filament. pH 7, image of the same purification fraction shown on the left adjusted to pH 7. (B) Ccrp58-Strep purified from *H. pylori*. (C) Strep-Ccrp1142 expressed in *E. coli*. (D) Electron microscopic image of solution buffer E. (E) Electron microscopic image of *H. pylori* wild-type (KE) fraction after Strep tag purification. All images are from PTA-stained samples. White scale bars, 100 nm.

ments *in vivo*. We therefore suggest the speculative model that all Ccrp proteins build up individual filaments. In this context it might be possible that different Ccrp polymers with different degrees of curvature may generate different degrees of helicity. However, whether the other Ccrp proteins generate mixed or individual filaments remains to be investigated.

In conclusion, *H. pylori* contains a complex cytoskeleton that affects cell morphology as well as motility.

We thank Ali Al-Ahmad for performing the statistical analysis and Maren Lingnau for technical assistance.

This work was supported by the Deutsche Forschungsgemeinschaft (WA2574/1-1, WA2574/1-2, and FOR 929).

REFERENCES

1. **Andersen, L. P.** 2007. Colonization and infection by *Helicobacter pylori* in humans. Helicobacter **12**(Suppl. 2)**:**12–15.
2. **Ausmees, N., J. R. Kuhn, and C. Jacobs-Wagner.** 2003. The bacterial cytoskeleton: an intermediate filament-like function in cell shape. Cell **115:**705–713.
3. **Baba, T., et al.** 2006. Construction of *Escherichia coli* K-12 in-frame, single-gene knockout mutants: the Keio collection. Mol. Syst. Biol. **2:**2006.0008.
4. **Bagchi, S., H. Tomenius, L. M. Belova, and N. Ausmees.** 2008. Intermediate filament-like proteins in bacteria and a cytoskeletal function in *Streptomyces*. Mol. Microbiol. **70:**1037–1050.

5. **Bonis, M., C. Ecobichon, S. Guadagnini, M. C. Prevost, and I. G. Boneca.** 2010. A M23B family metallopeptidase of *Helicobacter pylori* required for cell shape, pole formation and virulence. Mol. Microbiol. **78:**809–819.
6. **Cabeen, M. T., et al.** 2009. Bacterial cell curvature through mechanical control of cell growth. EMBO J. **28:**1208–1219.
7. **Defeu Soufo, H. J., et al.** 2010. Bacterial translation elongation factor EF-Tu interacts and colocalizes with actin-like MreB protein. Proc. Natl. Acad. Sci. U. S. A. **107:**3163–3168.
8. **Fiuza, M., et al.** 2010. Phosphorylation of a novel cytoskeletal protein (RsmP) regulates rod-shaped morphology in *Corynebacterium glutamicum*. J. Biol. Chem. **285:**29387–29397.
9. **Geis, G., S. Suerbaum, B. Forsthoff, H. Leying, and W. Opferkuch.** 1993. Ultrastructure and biochemical studies of the flagellar sheath of *Helicobacter pylori*. J. Med. Microbiol. **38:**371–377.
10. **Gerdes, S. Y., et al.** 2003. Experimental determination and system level analysis of essential genes in *Escherichia coli* MG1655. J. Bacteriol. **185:** 5673–5684.
11. **Go, M. F.** 2002. Review article: natural history and epidemiology of *Helicobacter pylori* infection. Aliment. Pharmacol. Ther. **16**(Suppl. 1)**:**3–15.
12. **Goldman, R. D., B. Grin, M. G. Mendez, and E. R. Kuczmarski.** 2008. Intermediate filaments: versatile building blocks of cell structure. Curr. Opin. Cell Biol. **20:**28–34.
13. **Helfand, B. T., L. Chang, and R. D. Goldman.** 2003. The dynamic and motile properties of intermediate filaments. Annu. Rev. Cell Dev. Biol. **19:**445–467.
14. **Herrmann, H., M. Haner, M. Brettel, N. O. Ku, and U. Aebi.** 1999. Characterization of distinct early assembly units of different intermediate filament proteins. J. Mol. Biol. **286:**1403–1420.
15. **Hoffman, P. S., et al.** 2003. Development of an interleukin-12-deficient mouse model that is permissive for colonization by a motile KE26695 strain of *Helicobacter pylori*. Infect. Immun. **71:**2534–2541.
16. **Josenhans, C., K. A. Eaton, T. Thevenot, and S. Suerbaum.** 2000. Switching of flagellar motility in *Helicobacter pylori* by reversible length variation of a short homopolymeric sequence repeat in fliP, a gene encoding a basal body protein. Infect. Immun. **68:**4598–4603.
17. **Kahrs, A. F., et al.** 1995. An improved TnMax mini-transposon system suitable for sequencing, shuttle mutagenesis and gene fusions. Gene **167:**53–57.
18. **Menard, A., A. Danchin, S. Dupouy, F. Megraud, and P. Lehours.** 2008. A variable gene in a conserved region of the *Helicobacter pylori* genome: isotopic gene replacement or rapid evolution. DNA Res. **15:**163–168.
19. **Pfeiffer, J., J. Guhl, B. Waidner, M. Kist, and S. Bereswill.** 2002. Magnesium uptake by CorA is essential for viability of the gastric pathogen *Helicobacter pylori*. Infect. Immun. **70:**3930–3934.
20. **Richard, H., and J. W. Foster.** 2004. *Escherichia coli* glutamate- and arginine-dependent acid resistance systems increase internal pH and reverse transmembrane potential. J. Bacteriol. **186:**6032–6041.
21. **Sarkar, G., and S. S. Sommer.** 1990. The "megaprimer" method of site-directed mutagenesis. Biotechniques **8:**404–407.
22. **Saunders, N. J., P. Boonmee, J. F. Peden, and S. A. Jarvis.** 2005. Interspecies horizontal transfer resulting in core-genome and niche-adaptive variation within *Helicobacter pylori*. BMC Genomics **6:**9.
23. **Schirm, M., et al.** 2003. Structural, genetic and functional characterization of the flagellin glycosylation process in *Helicobacter pylori*. Mol. Microbiol. **48:**1579–1592.
24. **Slomiany, B. L., and A. Slomiany.** 1992. Mechanism of *Helicobacter pylori* pathogenesis: focus on mucus. J. Clin. Gastroenterol. **14**(Suppl. 1)**:**S114–S121.
25. **Stingl, K., E. M. Uhlemann Em, G. Deckers-Hebestreit, R. Schmid, E. P. Bakker, and K. Altendorf.** 2001. Prolonged survival and cytoplasmic pH homeostasis of *Helicobacter pylori* at pH 1. Infect. Immun. **69:**1178–1180.
26. **Sycuro, L. K., et al.** 2010. Peptidoglycan crosslinking relaxation promotes *Helicobacter pylori*'s helical shape and stomach colonization. Cell **141:**822–833.
27. **Tomb, J. F., et al.** 1997. The complete genome sequence of the gastric pathogen *Helicobacter pylori*. Nature **388:**539–547.
28. **Waidner, B., et al.** 2002. Identification by RNA profiling and mutational analysis of the novel copper resistance determinants CrdA (HP1326), CrdB (HP1327), and CzcB (HP1328) in *Helicobacter pylori*. J. Bacteriol. **184:**6700–6708.
29. **Waidner, B., K. Melchers, F. N. Stahler, M. Kist, and S. Bereswill.** 2005. The *Helicobacter pylori* CrdRS two-component regulation system (HP1364/HP1365) is required for copper-mediated induction of the copper resistance determinant CrdA. J. Bacteriol. **187:**4683–4688.
30. **Waidner, B., et al.** 2009. A novel system of cytoskeletal elements in the human pathogen *Helicobacter pylori*. PLoS Pathog. **5:**e1000669.
31. **Zaar, K., et al.** 2002. Cellular and subcellular distribution of D-aspartate oxidase in human and rat brain. J. Comp. Neurol. **450:**272–282.